The creation and annihilation of optical vortices using cascade conical diffraction

D. P. O'Dwyer,[1] C. F. Phelan,[1] Y. P. Rakovich,[1] P. R. Eastham,[1] J. G. Lunney [1] and J. F. Donegan [1,2,*]

[1]*School of Physics, Trinity College Dublin, Dublin 2, Ireland*
[2]*Principal Investigator, CRANN Research Institute, Trinity College Dublin, Ireland.*
**jdonegan@tcd.ie*

Abstract: Internal conical diffraction produces a superposition of orthogonally polarised zero- and first-order Bessel like beams from an incident circularly polarised Gaussian beam. For right-circularly polarised light, the first-order beam has an optical vortex of charge −1. Upon propagation of the first-order beam through a second biaxial crystal, a process which is termed cascade conical refraction, the generated beam is a superposition of orthogonally polarised fields of charge 0 and −1 or 0 and −2. This spin to orbital angular momentum conversion provides a new method for the generation and annihilation of optical vortices in an all-optical arrangement that is solely dependent on the incident polarisation and vortex handedness.

OCIS codes: (350.5030) Phase; (260.1440) Birefringence; (260.1180) Crystal optics; (050.1940) Diffraction.

References and links

1. L. Allen, S. M. Barnett, and M. J. Padgett, *Optical angular momentum* (Bristol: Institute of Physics Publishing, (2003).
2. R. A. Beth, "Mechanical detection and measurement of the angular momentum of light," Phys. Rev. **50**(2), 115–125 (1936).
3. S. Franke-Arnold, L. Allen, and M. Padgett, "Advances in optical angular momentum," Laser Photon. Rev. **2**(4), 299–313 (2008).
4. R. L. Eriksen, P. J. Rodrigo, V. R. Daria, and J. Glückstad, "Spatial light modulator-controlled alignment and spinning of birefringent particles optically trapped in an array," Appl. Opt. **42**(25), 5107–5111 (2003).
5. C. Rotschild, S. Zommer, S. Moed, O. Hershcovitz, and S. G. Lipson, "Adjustable spiral phase plate," Appl. Opt. **43**(12), 2397–2399 (2004).
6. C. H. J. Schmitz, K. Uhrig, J. P. Spatz, and J. E. Curtis, "Tuning the orbital angular momentum in optical vortex beams," Opt. Express **14**(15), 6604–6612 (2006).
7. E. Karimi, B. Piccirillo, E. Nagali, L. Marrucci, and E. Santamato, "Efficient generation and sorting of orbital angular momentum eignmodes of light by thermally tuned q-plates," Appl. Opt. **94**, 231124 (2009).
8. S. Straupe, and S. Kulik, "Quantum optics: The quest for higher dimensionality," Nat. Photonics **4**(9), 585–586 (2010).
9. C. F. Phelan, D. P. O'Dwyer, Y. P. Rakovich, J. F. Donegan, and J. G. Lunney, "Conical diffraction and Bessel beam formation with a high optical quality biaxial crystal," Opt. Express **17**(15), 12891–12899 (2009).
10. M. V. Berry, M. J. Jeffrey, and M. Mansuripur, "Orbital and spin angular momentum in conical diffraction," J. Opt. A: Pure App. Opt. **7**, 685–690 (2005).
11. V. Peet, "Biaxial crystal as a versatile mode converter," J. Opt. **12**(9), 095706 (2010).
12. T. A. King, W. Hogervorst, N. S. Kazak, N. A. Khilo, and A. A. Ryzhevich, "Formation of higher-order Bessel light beams in biaxial crystals," Opt. Commun. **187**(4-6), 407–414 (2001).
13. M. Berry, "Conical diffraction asymptotics: Fine structure of Poggendorff rings and axial spike," J. Opt. A: Pure Appl. Opt. **6**, 289–300 (2004).
14. A. Abdolvand, K. G. Wilcox, T. K. Kalkandjiev, and E. U. Rafailov, "Conical refraction Nd:KGd$(WO^4)^2$ laser," Opt. Express **18**(3), 2753–2759 (2010).
15. M. V. Berry, "Conical diffraction from an N-crystal cascade," J. Opt. **12**(7), 075704 (2010).
16. D. P. O'Dwyer, C. F. Phelan, Y. P. Rakovich, P. R. Eastham, J. G. Lunney, and J. F. Donegan, "Generation of continuously tunable fractional optical orbital angular momentum using internal conical diffraction," Opt. Express **18**(16), 16480–16485 (2010).

#140074 - $15.00 USD Received 22 Dec 2010; revised 10 Jan 2011; accepted 17 Jan 2011; published 26 Jan 2011

17. A. Vaziri, J. W. Pan, T. Jennewein, G. Weihs, and A. Zeilinger, "Concentration of higher dimensional entanglement: qutrits of photon orbital angular momentum," Phys. Rev. Lett. **91**(22), 227902 (2003).
18. S. S. R. Oemrawsingh, X. Ma, D. Voigt, A. Aiello, E. R. Eliel, G. W. Hooft, and J. P. Woerdman, "Experimental demonstration of fractional orbital angular momentum entanglement of two photons," Phys. Rev. Lett. **95**(24), 240501 (2005).
19. E. Karimi, J. Leach, S. Slussarenko, B. Piccirillo, L. Marrucci, L. Chen, W. She, S. Franke-Arnold, M. J. Padgett, and E. Santamato, "Spin-orbit hybrid entanglement of photons and quantum contextuality," Phys. Rev. A **82**(2), 022115 (2010).
20. L.-P. Deng, H. Wang, and K. Wang, "Quantum CNOT gates with orbital angular momentum and polarisation of single-photon quantum logic," J. Opt. Soc. Am. B **24**(9), 2517–2520 (2007).
21. L. Chen, and W. She, "Increasing Shannon dimensionality by hyperentanglement of spin and fractional orbital angular momentum," Opt. Lett. **34**(12), 1855–1857 (2009).

1. Introduction

The total angular momentum of a paraxial beam of light consists of a spin component associated with polarisation and an orbital component due to the presence of a helical phase structure [1]. For a left- or right-circularly polarised beam, the spin angular momentum (SAM) is ±ħ per photon [2]. Orbital angular momentum (OAM) can arise in beams containing optical vortices, associated with an azimuthal phase factor $e^{i\ell\theta}$. The integer ℓ is the vortex topological charge, where $2\pi\ell$ is the phase change around the beam axis [1, 3]. The presence of an optical vortex implies a point of zero intensity around which the phase winds. For a scalar beam with an azimuthally uniform intensity profile the OAM per photon is ℓħ, so that the quantization of vortex charge implies quantization of OAM. In a general beam, however, the expectation value of the OAM per photon is not related to the vortex charge [4].

The polarisation, and hence the SAM, of a beam of light is easily changed by using a quarter-wave plate. The generation of light beams with controllable OAM requires a new set of optical devices to manipulate the azimuthal phase distribution of the beam. Common devices include spatial light modulators (SLM) [4], spiral phase plates (SPP) [5] and computer generated holograms (CGH) [6]. They are all widely tuneable, enabling access to integer or non-integer OAM values, with non-integer values corresponding to superpositions of beams of different vortex charge. However, these devices also have their associated problems such as low mode conversion efficiency (SLM, CGH), cost (SLM), and mode quality (SPP, CGH).

An alternative approach to creating beams with tunable OAM is to tune the SAM and then convert SAM to OAM. This has the advantage that the SAM is readily tunable using standard optical components that manipulate the polarisation. Recent publications on the conversion of SAM into OAM using q-plates show the interest in such polarisation controlled devices in the fields of quantum optics and quantum communications [7-8]. A q-plate has been used to convert a circularly polarised light beam with $\sigma = +1\hbar$ to a beam with $\ell = +2\hbar$ with a very high efficiency (up to ≈98%), but can have problems with mode quality [7].

Several groups have shown internal conical diffraction (ICD) using a single biaxial crystal provides an efficient means for the conversion of circularly polarised Gaussian modes ($\sigma = \pm 1\hbar$) into a superposition of high quality Bessel-like beams with $\ell = 0$ and $\ell = \pm 1$, with a net ± ½ħ OAM per photon [9–12]. Using ICD of elliptically polarised light and filtering of the resulting beam allows the generation of a beam in which the OAM can be continuously tuned between 0 and ± ħ per photon [14]. In this paper, we show that a cascade of two biaxial crystals, with intervening polarisers, can be used to generate beams with $\ell = \pm 1$ or ± 2. The approach can be generalized to an arbitrary number of crystals, providing a polarisation-tunable system for creating a wide variety of high-order vortex beams. Such beams may find applications in quantum information processing, and in studies of the propagation of optical singularities.

#140074 - $15.00 USD Received 22 Dec 2010; revised 10 Jan 2011; accepted 17 Jan 2011; published 26 Jan 2011

King et al. [12] have described the theoretical analysis and experimental observation of zero-to-second order transformation of a non-diverging Bessel beam using ICD in a two crystal configuration, including a measurement of the radial intensity profile. In this paper we report the measurement of the phase profiles resulting from ICD in a two-crystal cascade, explicitly showing the generation of a doubly charged vortex. In addition, we compare the measured radial intensity profiles with the predictions of a paraxial approximation calculation of the propagation of a Gaussian laser beam through a cascade of two crystals. More recently, Berry formulated the theory of ICD in a cascade of *n* biaxial crystals of arbitrary lengths and with arbitrary azimuthal orientations [15]. This work did not consider the effect of changing the state of polarisation between crystals, which is one of the topics considered in our work.

2. Theory of cascade conical refraction

Internal conical diffraction (ICD) occurs when a narrow light beam is incident along an optic axis of a biaxial crystal, with refractive indices $n_1 < n_2 < n_3$. This incident beam is refracted into a cone inside the crystal, and emerges as a hollow cylinder. As discussed by Berry [13], in the paraxial approximation, the incident field profile transforms according to:

$$\mathbf{E}(\mathbf{R},Z)=\frac{k}{2\pi}\iint e^{ik(\mathbf{P}\cdot\mathbf{R}-\frac{1}{2}ZP^2)}\times[\cos(kPR_0)\mathbf{I}-i\sin(kPR_0)\mathbf{M}(\theta_P)]\mathbf{a}(\mathbf{P})d\mathbf{P} \qquad (1)$$

with

$$\mathbf{M}(\theta_P)=\begin{pmatrix}\cos\theta_P & \sin\theta_P\\ \sin\theta_P & -\cos\theta_P\end{pmatrix} \qquad (2)$$

Here **R** is the transverse cone-centred position, $k\mathbf{P}=k(P_x,P_y)=kP(\cos\theta_\mathbf{P},\sin\theta_\mathbf{P})$ is the transverse wave vector, **I** is the identity matrix, and $k = n_2k_0$ is the crystal wave-number. R_0 is the radius of the cylindrical beam emerging from the crystal. When the input beam is focussed on the entrance face of the crystal the variable Z in Eq. (1) which describes the propagation distance is defined as $Z = L + (z\text{-}L)n_2$, where L is the length of the crystal and z is the distance from the entrance face. The components of **a(P)** are Fourier representations of the Cartesian components of the field incident on the entrance face. For the case of a Gaussian beam which is focussed to form a beam waist at some other position, **a(P)** may be taken to be the field at the waist and z measured from its location. In the alternative basis of circularly-polarised fields, with Jones vectors $(1, \pm i)/\sqrt{2}$, the matrix $\mathbf{M}(\theta_p)$ is replaced by

$$\mathbf{M}(\theta_P)=\begin{pmatrix}0 & e^{-i\theta_P}\\ e^{i\theta_P} & 0\end{pmatrix} \qquad (3)$$

From Eqs. (1) and (3) it can be see that a circularly-polarised beam becomes a superposition of a component of the same circular polarisation, and a component with the opposite polarisation and an azimuthal phase factor. This factor results in an optical vortex of the same charge as the incident helicity; +1 for left-circular and −1 for right-circular polarisation. More explicitly, conical diffraction of a uniform left- (right-) polarised beam generates a superposition of two Bessel-like beams of zero (B_0) and first order (B_1)

$$\mathbf{E}(R,Z)=B_0(R,R_0,Z)\mathbf{e}^{+(-)}+B_1(R,R_0,Z)e^{+(-)i\theta}\mathbf{e}^{-(+)} \qquad (4)$$

$$B_0(R,R_0,Z)=k\int_0^\infty P\cos(kPR_0)a(P)J_0(kPR)e^{-\frac{1}{2}ikP^2Z}dP, \qquad (4a)$$

$$B_1(R,R_0,Z)=k\int_0^\infty P\sin(kPR_0)a(P)J_1(kPR)e^{-\frac{1}{2}ikP^2Z}dP, \qquad (4b)$$

#140074 - $15.00 USD Received 22 Dec 2010; revised 10 Jan 2011; accepted 17 Jan 2011; published 26 Jan 2011

where $\mathbf{e}^{-(+)}$ denotes right- (left-) circular polarisation, and we have assumed that the incident beam is circularly symmetric. The individual profiles B_0 and B_1 satisfy the paraxial wave equation and have been shown experimentally to agree with theory [9].

In cascade conical diffraction, a beam propagates through a series of biaxial crystals. This process has recently been exploited in lasers with increased efficiency and novel beam shapes [14] and treated theoretically by Berry [15]. Additionally, by manipulating the polarisation state between the crystals in the cascade, a wide variety of beams of varying vorticity can be generated. In our experiments, we consider a two-crystal cascade whose optical axes are aligned, in which only one of the circular components after the first crystal (see Eq. (4)) is transmitted into the second, which we assume to be of equal length for simplicity. Suppose first that only the circularly polarised B_1 beam is incident on the second crystal. If the beam into the first crystal is right-circular then B_1 is left-circularly polarised, and can be isolated with a left-circular polarizer. Its Fourier representation is

$$\mathbf{a}(\mathbf{P}) = -ie^{-\frac{1}{2}ikP^2Z}\sin(kPR_0)\mathbf{M}(\theta_p)a_{in}(P)\mathbf{e}^- = -ie^{-\frac{1}{2}ikP^2Z}\sin(kPR_0)e^{-i\theta_P}a_{in}(P)\mathbf{e}^+ \quad (5)$$

where $a_{in}(P)$ is the Fourier representation of the radial profile of the beam that was incident on the first crystal. Substituting Eq. (5) into Eq. (1) and performing the Fourier transformation back to real space gives the output field

$$\mathbf{E}(R,\theta,Z) = B_{12}e^{-i\theta}\,\mathbf{e}^+ + B_{02}\mathbf{e}^- \quad (6)$$

$$B_{02} = \frac{k}{2}\int_0^\infty P(\cos(2kPR_0)-1)a_{in}(P)J_0(kPR)e^{-\frac{1}{2}ikP^2Z_2}dP \quad (6a)$$

$$B_{12} = \frac{k}{2}\int_0^\infty P\sin(2kPR_0)\,a_{in}(P)J_1(kPR)e^{-\frac{1}{2}ikP^2Z_2}dP \quad (6b)$$

Here $Z_2=2L+(z-2L)n_2$ where 2L is the total length of the crystals in the cascade. In labelling the output beam components the first subscript refers to the order of the Bessel function occurring in the description of that field component and the second subscript refers to the number of crystals used. It can be seen that the output from the second crystal is a superposition of a left-circular zero-order Bessel like beam and a right-circular first-order beam. Thus for the part of the output beam the vortex present in the input has been annihilated by the action of the second crystal.

If, after isolating the B_1 beam, we right-circularly polarize it, its Fourier transform is

$$\mathbf{a}(\mathbf{P}) = -ie^{-\frac{1}{2}ikZP^2}\sin(kPR_0)e^{-i\theta_P}a_{in}(P)\mathbf{e}^-, \quad (7)$$

and the field emerging from the second crystal is

$$\mathbf{E}(R,\theta,Z) = B_{12}e^{-i\theta}\mathbf{e}^- + B_{22}e^{-2i\theta}\mathbf{e}^+, \quad (8)$$

where

$$B_{22} = \frac{k}{2}\int_0^\infty P(1-\cos(2kPR_0))\,a_{in}(P)J_2(kPR)e^{-\frac{1}{2}ikP^2Z_2}dP \quad (8a)$$

The B_{22} component contains a vortex of charge two, thus the action of the second crystal is to increase the vorticity of the beam entering it.

The beam from a *n*-crystal cascade [15] can be constructed from Eq. (1). After each crystal the field will have a Fourier representation with components of the form

$$\mathbf{a}(\mathbf{P}) = a(P)e^{in\theta_P}\mathbf{e}^{+(-)} \quad (9)$$

#140074 - $15.00 USD Received 22 Dec 2010; revised 10 Jan 2011; accepted 17 Jan 2011; published 26 Jan 2011

corresponding to the real-space beams

$$\mathbf{E}(R,\theta,Z) = i^n e^{in\theta}\mathbf{e}^{+(-)}k\int_0^\infty PJ_n(kPR)a(P)dP \tag{10}$$

A subsequent conical diffraction stage transforms such a beam into

$$e^{-\frac{1}{2}ikP^2Z}\left\{\cos(kPR_0)a\ (P)e^{in\theta_P}\mathbf{e}^{+(-)} - i\ \sin(kPR_0)e^{-i\theta_P}a\ (P)e^{i(n+(-)1)\theta_P}\mathbf{e}^{+(-)}\right\} \tag{11}$$

which is again a superposition of components of the form of Eq. (5), generating new radial profiles *a'(P)*, vorticities *n*', and polarisations. The output beam from a cascade is obtained by iterating the transformation of Eq. (11) for each stage in the cascade, and Fourier transforming the final Fourier components using Eq. (10). Figure 1 shows a pictorial representation of the cascade process in which the various outputs are shown.

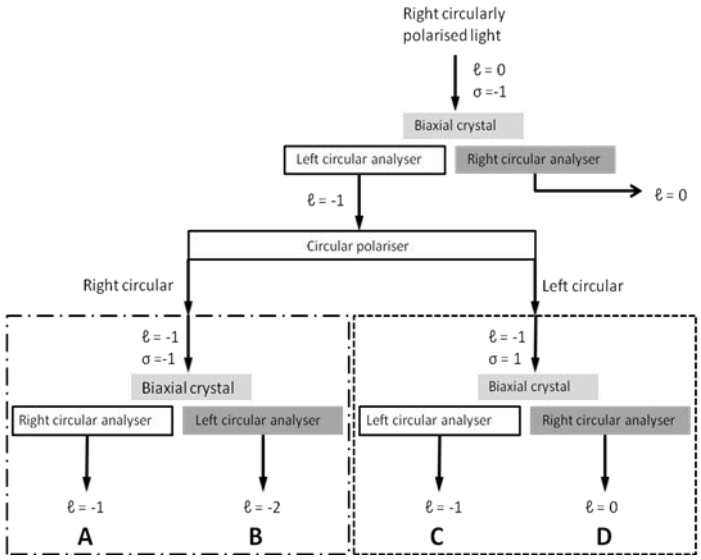

Fig. 1. Schematic diagram of the cascade conical refraction process. Outputs A,B,C and D are discussed in the text.

3. Experimental results and discussion

The experimental setup for two-crystal cascade conical diffraction is shown in Fig. 2. The biaxial crystals used were $KGd(WO_4)_2$, $n_1 = 2.013$ $n_2 = 2.045$ $n_3 = 2.086$ and the semi-cone angle of the rays in the crystal is A = 0.0196 rad. A 10 mW HeNe Gaussian laser mode at 632.8mn is right-circularly polarised using a λ/4 plate, focused to a beam waist size *w* of 41 μm at the $1/e^2$ point using a 5 cm lens (L), and propagated along the optic axis of the biaxial crystal. The first crystal used had a length L_1 = 20.9 mm resulting in $R_0 = AL_1 = 0.0410$ mm for the radius of the double ring in the focal image plane, which is the plane where the double ring is most clearly defined. The SAM to OAM conversion efficiency was calculated by Berry [10] and is directly correlated to the strength of the crystal, this is quantified as the conical quality term $\rho_o = (AL_1/w)$; for the first crystal ρ_o = 10.0. For this large value of ρ_o, ICD of a circularly polarised beam results in an almost equal division of the optical power between the B_0 and B_1 components [13]. The circularly polarised light with ($\sigma = \pm 1\hbar$) is converted into a superposition of OAM states with $\ell = 0$ and $\ell = \pm 1\hbar$ giving a net OAM of $\ell = \pm \frac{1}{2}\hbar$ per photon. As shown in Fig. 1 the field component isolated by the circular analyser following the first crystal is again circularly polarised using another

#140074 - $15.00 USD Received 22 Dec 2010; revised 10 Jan 2011; accepted 17 Jan 2011; published 26 Jan 2011

quarter wave-plate and propagates along the optic axis of the second biaxial crystal. This crystal had a length of L_2 = 21.0 mm and a R_0 value of 0.0415 mm giving a R_0' value of 0.0825 mm and a net ρ_o = 20.0 for ICD in the two-crystal cascade.

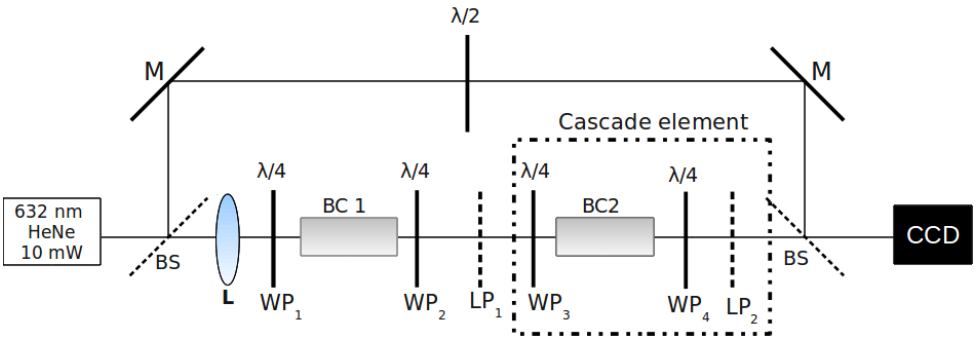

Fig. 2. Optical setup for cascade conical diffraction, including a Mach-Zehnder interferometer. The cascade element is removed to enable the imaging of the profiles from the first crystal. BS - beam splitters, M - Mirrors, $WP_{1/2/3/4}$ are λ/4 plates, $LP_{1/2}$ are linear polarisers. λ/2 plate is used to rotate the Gaussian reference arm polarisation to match the polarisation of the conical field.

A Mach-Zehnder interferometer is used to examine the phase distribution of the generated conical beams and reveal the presence and charge of any optical vortices present. The polarisation of the Gaussian beam in the reference arm of the interferometer was rotated using a half-wave plate to match the linear polarisation of the conically diffracted beam component under examination. When a beam with a helical wave is collinearly interfered with a Gaussian beam that has a wavefront with different curvature, a spiral fringe pattern is observed; the number of interlacing spirals equals the charge of the optical vortex. If on the other hand, the beams are slightly misaligned a wedge interference pattern of parallel fringes with an edge dislocation of one or more fringes is seen. The number of extra fringes terminating on the dislocation equals the number of 2π azimuthal phase changes around the beam axis, or the charge of the optical vortex [3].

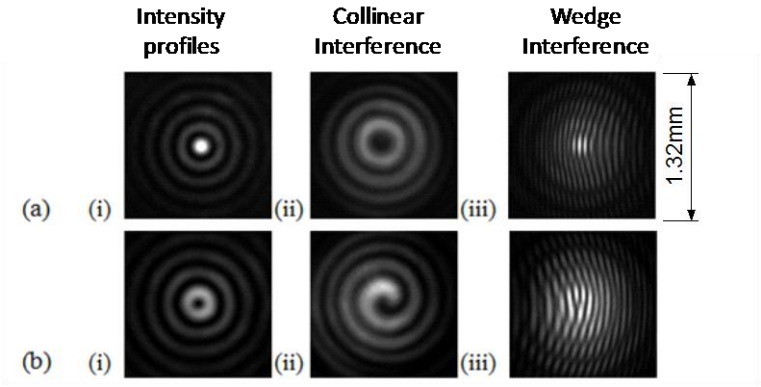

Fig. 3. Far-field intensity patterns of separated conically diffracting beam described by a Bessel function after first biaxial crystal. (a) (i) zero-order conically diffracting Bessel beam (ii) collinear interference pattern with a Gaussian beam (iii) wedge interference pattern. (b) first-order diffracting Bessel beam (ii) collinear interference pattern with a Gaussian beam (iii) wedge interference pattern showing first order edge dislocation. All images are 1.32 mm x 1.32 mm in size.

Both the radial intensity distributions and the interference patterns were recorded on a standard CCD camera in the far-field region of the conically diffracted beam, 39 cm away

#140074 - $15.00 USD Received 22 Dec 2010; revised 10 Jan 2011; accepted 17 Jan 2011; published 26 Jan 2011

from the focal image plane [9]. Upon exiting the first crystal the orthogonal fields are separated with a λ/4 plate (WP_2) and linear polariser (LP_1).

Figure 3 shows the intensity distributions and interference patterns for the B_0 (a) and B_1 (b) beams arising from conical diffraction from a single crystal (with the cascade element removed). As expected the zero-order Bessel like beam (Fig. 3(a)) shows an intensity maximum at the centre and azimuthally uniform phase. For the first order beam (Fig. 3(b(i))) there is a zero intensity on axis. The single spiralling fringe and single edge dislocation in the wedge interference confirms the presence of an optical vortex of charge −1.

To examine the features of the two-crystal conical diffraction the cascade element is inserted in the optical setup as shown in Fig. 2. The B_1 component (Fig. 3(b)) was selected and circularly polarised using WP_3 before entering the second crystal. Various outputs beams are obtained depending on the setting of WP_3 to generate left- or right-circular polarisation and the setting of the output analyser (WP_4 and LP_2) to select left- or right-circularly polarised light.

Before describing the various output beams we should recall that the polarisation into the first crystal is right-circular. Now setting the polarisation of the B_1 beam into the second crystal to be right-circular and setting the output analyser to be right-circular yields the intensity distribution and interference patterns shown in Fig. 4. These indicate a vortex beam of charge −1 corresponding to B_{12} (Eq. (6)b) and output A in Fig. 1. If the output analyser is set left-circular the intensity distribution and interference patterns shown in Fig. 5 are observed, which correspond to a vortex beam with $\ell = -2$, i.e. B_{22} (Eq. (8)a) and output B in Fig. 1. In this case the second crystal is acting to increase the charge of the optical vortex by 1. On the other hand if the polarisation of the B_1 beam into the second crystal is set left-circular and the output analyser is set to transmit right-circular the intensity distribution and interference patterns are as shown in Fig. 6. Clearly this beam does not contain an optical vortex and corresponds to output D in Fig. 1. If the output analyser is adjusted to transmit left circular (output C Fig. 1) the intensity distribution and interference patterns are the same as Fig. 4, which is a B_{12} beam. We can generalise the operation of the second conical refraction step by noting that with the input beam with OAM of $\ell\hbar$ per photon, we can, by suitable choice of input circular polarisation and handedness of the output analyser, generate beams with $(\ell-1)\hbar$, $\ell\hbar$ and $(\ell+1)\hbar$ per photon.

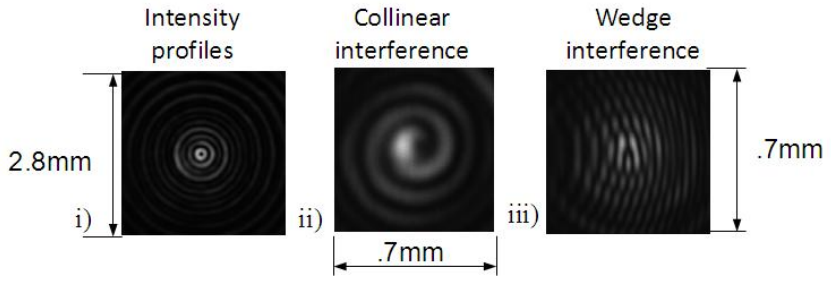

Fig. 4. $\ell = -1$ component of Path A and Path C from Fig. 1.(i) intensity profile (ii) collinear interference with a Gaussian beam (iii) wedge interference with a Gaussian beam.

#140074 - $15.00 USD Received 22 Dec 2010; revised 10 Jan 2011; accepted 17 Jan 2011; published 26 Jan 2011

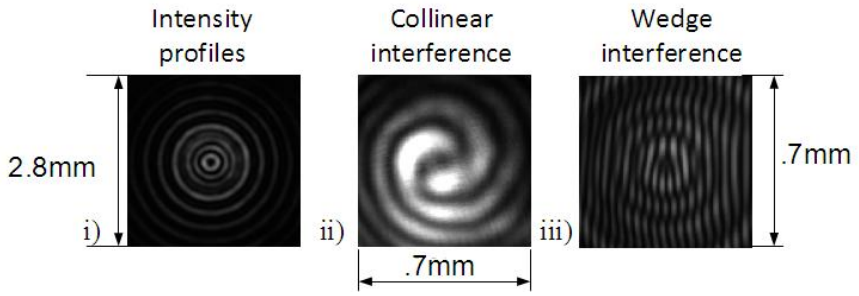

Fig. 5. $\ell = -2$ component of Path B from Fig. 1. (i) intensity profile (ii) collinear interference with a Gaussian beam (iii) wedge interference with a Gaussian beam

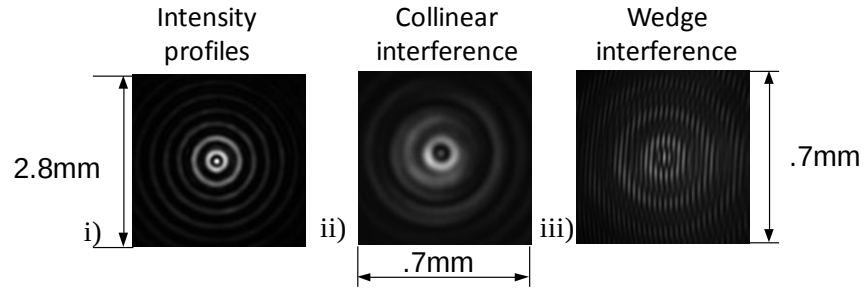

Fig. 6. $\ell = 0$ component of Path D from Fig. 1. (i) Intensity profile (ii) collinear interference with a Gaussian beam (iii) wedge interference with a Gaussian beam

The various radial intensity profiles resulting from the two crystal conical diffraction were examined in more detail and compared with calculation according to the paraxial approximation. This comparison is shown in Fig. 7 where the calculated profile is normalised to the first maximum. Images of the calculated intensity distributions are also shown. In all three cases there is quite good agreement between theory and experiment in terms of the radial location of the maxima.

The work reported here using cascade conical diffraction together with relatively simple polarisation optics to switch between different optical OAM states may find application in the field of quantum information processing [17–21]. Coupled with the previous work on the generation of beams with fractional OAM using elliptically polarised light [16], it seems that internal conical diffraction provides a flexible and high fidelity technique for the generation and control of optical OAM.

#140074 - $15.00 USD Received 22 Dec 2010; revised 10 Jan 2011; accepted 17 Jan 2011; published 26 Jan 2011

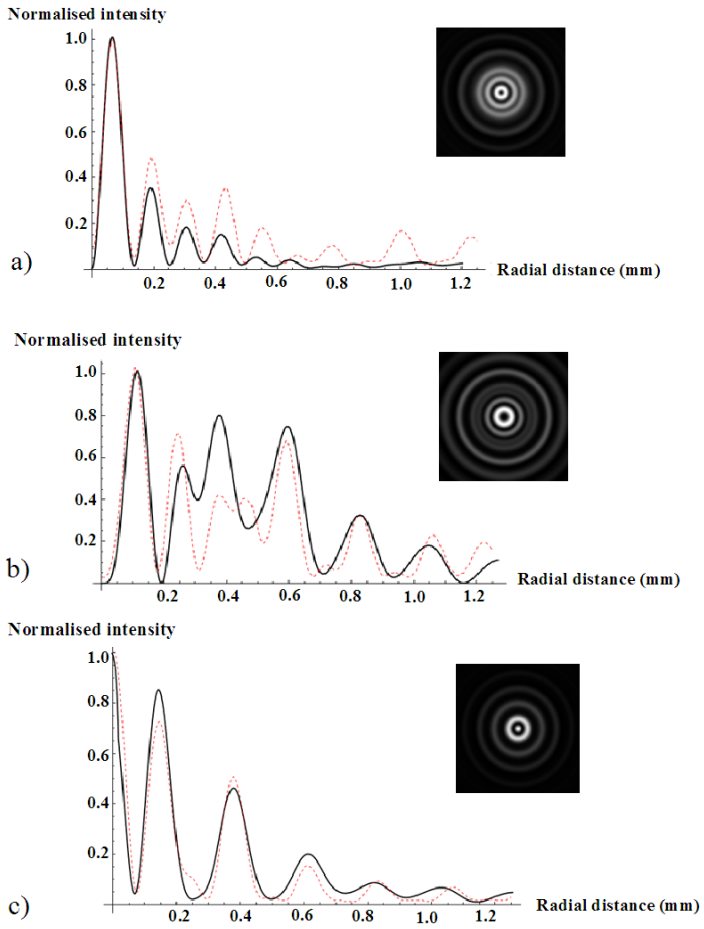

Fig. 7. Measured (dashed) and calculated (solid) radial intensity profiles of (a) B_{12}, (b) B_{22} and (c) B_{02} beams generated in a two crystal cascade internal conical diffraction process. Calculated images of the intensity distribution are also shown.

4. Conclusion

Using internal conical diffraction in a two biaxial crystal cascade together with some simple polarisation optics we have demonstrated the generation of optical vortices with topological charge of ±1 and ±2. We have also demonstrated raising and lowering of the order of an optical vortex, including the annihilation of an optical vortex of charge ±1. In principle, our two crystal experiment can be extended to *n* biaxial crystals to generate optical vortices with a maximum charge *n*, though there is 50% power loss for each successive cascade element added.

Acknowledgements

We acknowledge the support of Science Foundation Ireland under research grants 06/RFP/PHY029, SFI/SIRG/I1592 and 08/IN.1/I1862 and Sir Michael Berry for helpful discussions.

#140074 - $15.00 USD Received 22 Dec 2010; revised 10 Jan 2011; accepted 17 Jan 2011; published 26 Jan 2011